REGULAR ARTICLE

blood advances

CD158k and PD-1 expressions define heterogeneous subtypes of Sezary syndrome

Inès Vergnolle,[1] Claudia Douat-Beyries,[1] Serge Boulinguez,[2] Jean-Baptiste Rieu,[1] Jean-Philippe Vial,[3] Rolande Baracou,[1] Sylvie Boudot,[1] Aurore Cazeneuve,[1] Sophie Chaugne,[1] Martine Durand,[1] Sylvie Estival,[1] Nicolas Lablanche,[1] Marie-Laure Nicolau-Travers,[1] Emilie Tournier,[4] Laurence Lamant,[4,5] and François Vergez[1,5,6]

[1]Laboratoire d'Hématologie, Centre Hospitalier Universitaire de Toulouse, Institut Universitaire du Cancer de Toulouse Oncopole, Toulouse, France; [2]Service de Dermatologie, CHU Toulouse, Toulouse, France; [3]Laboratoire d'Hématologie, Centre Hospitalier Universitaire de Bordeaux, Bordeaux, France; [4]Laboratoire d'Anatomopathologie, Institut Universitaire du Cancer de Toulouse Oncopole, CHU Toulouse, Toulouse, France; [5]Université Toulouse III Paul Sabatier, Toulouse, France; and [6]Cancer Research Center of Toulouse, UMR1037 INSERM, ERL5294 French National Centre for Scientific Research, Toulouse, France

Key Points

- SS can be divided into 3 subtypes, each with a different immune environment and response to treatment.

Sezary syndrome (SS) is a rare leukemic form of cutaneous T-cell lymphoma. Diagnosis mainly depends on flow cytometry, but results are not specific enough to be unequivocal. The difficulty in defining a single marker that could characterize Sezary cells may be the consequence of different pathological subtypes. In this study, we used multivariate flow cytometry analyses. We chose to investigate the expression of classical CD3, CD4, CD7, and CD26 and the new association of 2 markers CD158k and PD-1. We performed lymphocyte computational phenotypic analyses during diagnosis and follow-up of patients with SS to define new SS classes and improve the sensitivity of the diagnosis and the follow-up flow cytometry method. Three classes of SS, defined by different immunophenotypic profiles, $CD158k^+$ SS, $CD158k^-PD\text{-}1^+$ SS, CD158k and PD-1 double-negative SS, showed different $CD8^+$ and B-cell environments. Such a study could help to diagnose and define biological markers of susceptibility/resistance to treatment, including immunotherapy.

Introduction

Sezary syndrome (SS) is a rare leukemic form of cutaneous T-cell lymphoma (CTCL), defined by erythroderma, pruritus, lymphadenopathy, and clonal T cells in the skin, lymph nodes, and peripheral blood. SS accounts for <5% of CTCL, occurs in aged adults, and has a male predominance.

SS, mycosis fungoides (MF), and erythrodermic inflammatory diseases share overlapping clinical and biological features, often making diagnosis difficult. Because prognosis differs between diseases, defining and harmonizing the diagnosis process have been a real challenge for many years.[1]

Blood tumor burden evaluation mainly depends on the detection of Sezary cells by flow cytometry (FC) but results are not specific enough to be unequivocal.[2,3]

Currently, flow cytometry is used to quantify $CD4^+$ lymphocyte subpopulations that lack T-cell marker expression, such as CD7 and CD26 (International Society for Cutaneous Lymphomas, ISCL).[3,4] Thus, because of the low specificity of these univariate criteria, the diagnostic thresholds are high (either 40% of $CD4^+CD7^-$ or 30% of $CD4^+CD26^-$ or respective absolute count >1000/μL).

Submitted 3 May 2021; accepted 23 July 2021; prepublished online on *Blood Advances* First Edition 27 September 2021; final version published online 16 March 2022. DOI 10.1182/bloodadvances.2021005147.

Requests for data sharing may be submitted to Ines Vergnolle (vergnolle.ines@iuct-oncopole.fr).

The full-text version of this article contains a data supplement.

Table 1. Biological and clinical characteristics at first sampling of patients with SS

Number	Sex	Age (y)	Date of first sampling	Date of diagnosis	ISCL stage	Sezary cells (microscopic count, %)	Lymphocytosis (/μL)	Treatment at first sampling	Treatments	Skin biopsy
SS1	M	66	16/12	17/01	B1	7	2 533	None	Phototherapy, MTX, ECP	Nonspecific
SS2	M	68	18/02	17/10	B2	49	15 161	None	MTX, ECP	Nonspecific
SS3	F	66	20/11	20/01	B2	76	6 414	None	MTX, MTX + ECP	Specific
SS4	F	63	17/08	17/09	B2	<1	2 394	None	MTX, ECP + MTX, ECP + Bexarotene	Nonspecific
SS5	M	73	17/01	12/08	B1	ND	914	ECP	MTX, ECP	ND
SS6	M	75	17/01	16/05	B1	18	1 730	None	Bexarotene, Bexarotene + ECP	ND
SS7	F	89	17/06	17/06	B2	24	5 009	None	MTX, none	Nonspecific
SS8	M	80	16/09	15/09	B0	ND	549	None	Bexarotene, ECP	Nonspecific
SS9	F	85	19/04	19/04	B2	32	4 558	None	None	Nonspecific
SS10	F	66	17/05	17/05	B1	3	2 465	None	Photothérapy, ECP	Nonspecific
SS11	F	68	18/08	18/08	B2	30	5 102	None	MTX, ECP	Nonspecific
SS12	F	87	18/11	18/11	B2	85	58 878	None	MTX, ECP + MTX, ECP	Specific
SS13	M	63	17/02	15/05	B1	ND	1 376	ECP	ECP + MTX	Specific
SS14	F	60	20/02	20/02	B2	51	15 023	None	MTX, MTX + ECP	Nonspecific
SS15	F	87	19/01	19/01	B2	54	12 326	None	MTX, ECP, none (CR)	Nonspecific
SS16	M	75	16/01	16/06	B2	7	5 168	None	MTX, MTX + ECP, phototherapy, bexarotene, mogamulizumab	Nonspecific
SS17	M	91	16/07	16/07	B2	ND	11 934	None	Phototherapy, MTX, acitretin	Specific
SS18	M	73	18/02	18/02	B1	ND	2 541	None	Phototherapy, MTX, acitretin, bexarotene, ECP+ bexarotene, mogamulizumab interferon	Nonspecific

ECP, extracorporeal photophoresis; F, female; M, male; MTX, methotrexate; ND, not done.

Several studies have focused on the discovery of SS hallmarks. T central memory cell markers have been investigated because of assumed cell of origin of SS (CCR7, CD27, CD45RO, CD45RA, CD62, CD95, and CD103).[5,6] Finally, percentage of peripheral T central memory cells in patients with SS is variable, and SS cells exhibit a phenotypic plasticity for these markers. Skin homing receptor studies showed similar results (CCR4, CCR6, CCR10, CXCR3, and CLA).[5,6] Others have identified an expansion of a $CD60^{+}CD26^{-}CD49d^{-}$ T-cell clone in Patients with SS, but they used only 10 healthy donors as controls.[7] A study performed in 8 Patients with SS screened 240 markers and concluded heterogeneity in surface marker expression.[8] The high difficulty in defining a single marker that could characterize SS may be the consequence of different pathological subtypes.

Nevertheless, a few markers seemed promising, like KIR3DL2/CD158k and PD-1/CD279.[2,9]

KIR3DL2/CD158k is a member of the killer cell immunoglobulin-like receptor (KIR), identified by transcriptomic analyses. It was described as a reliable SS^{+} marker, but some studies suggested a lack of sensitivity and the need for further studies in normal $CD4^{+}$ T cells.[2,3,9,10] Similarly, PD-1/CD279 is nearly systematically expressed in skin biopsies of patients with SS in contrast to MF cases.[11] A study on peripheral lymphocytes confirmed these data but only on a few patients.[12]

In this study, leaving aside the classical biphenotypic analysis, we proposed a new approach using unsupervised multivariate FC analyses. We chose to investigate the expression of classical CD3, CD4, CD7, and CD26 and the new association of the 2 markers CD158k and PD-1/CD279. We performed lymphocyte computational phenotypic analyses during diagnosis and follow-up of patients with SS to better define Sezary cells and improve the sensitivity of the diagnostic and follow-up FC method.[13]

Materials and methods

Patients

Peripheral blood cells from 231 patients admitted to the dermatology department of Toulouse University Hospital between 2015 and 2020 were assessed: 18 patients with SS, 39 patients with MF, 18 patients with other CTCL (without circulating lymphoma T cells), and 156 patients without CTCL (mainly erythrodermic inflammatory diseases or B-cell lymphomas). Patients were classified according to their complete medical records and final clinical diagnosis.

A full list of SS patient characteristics, including treatments, is shown in Table 1. The study was conducted in accordance with the Declaration of Helsinki.

FC

Fresh samples were analyzed at diagnosis and/or at different time points during the follow-up. Ten-color labeling was performed with

Table 2. Other CTCL

CTCL	Number
Anaplastic large cell lymphoma	6
Peripheral T-cell lymphoma, not otherwise specified	2
Lymphomatoid papulosis	3
Subcutaneous panniculitis-like T-cell lymphoma	2
Other CTCLs	5

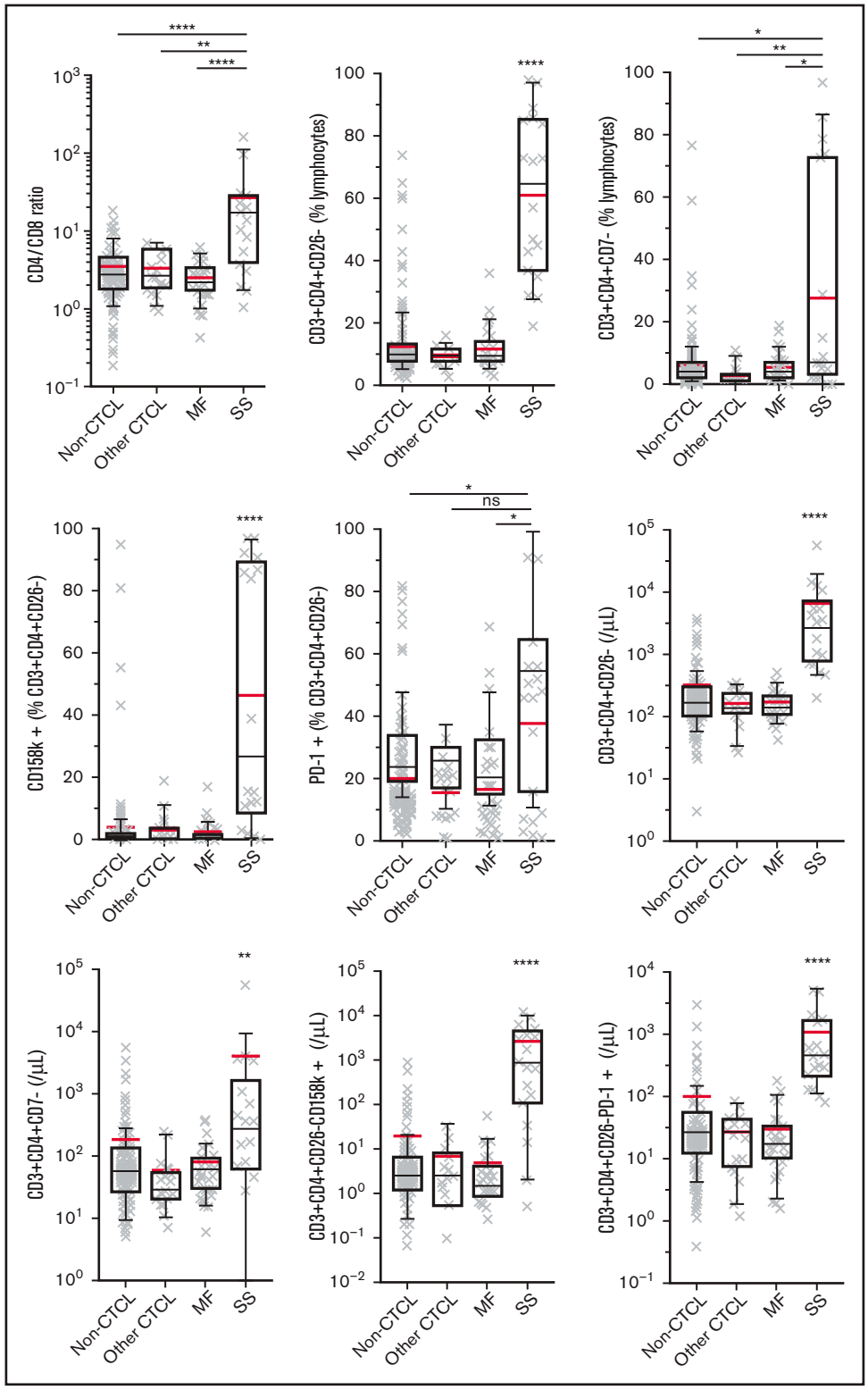

Figure 1. ISCL criteria and CD158k and PD-1 expressions on $CD4^+CD26^-$ cells. (A) The CD4/CD8 ratio in patients without CTCL (non-CTCL; n = 156), with another type of CTCL (CTCL; n = 18), with MF (n = 39) or with SS (n = 18). (B) Percentage of $CD4^+CD26^-$ lymphocytes (n = 156, n = 18, n = 39, n = 18, respectively). (C) Percentage of $CD4^+CD7^-$ lymphocytes (n = 155, n = 18, n = 39, n = 18, respectively). (D) Percentage of $CD158k^+$ SS-like cells (n = 149, n = 18, n = 39, n = 18, respectively). (E) Percentage of $PD\text{-}1^+$ SS-like cells (n = 122, n = 18, n = 36, n = 18, respectively). (F) Absolute values of $CD4^+CD26^-$ lymphocytes (n = 156, n = 18, n = 39, n = 18, respectively). (G) Absolute values of $CD4^+CD7^-$ lymphocytes (n = 155, n = 18, n = 39, n = 18, respectively). (H) Absolute values of $CD158k^+$ SS-like cells (n = 149, n = 18, n = 39, n = 18, respectively). (I) Absolute values of $PD\text{-}1^+$ SS-like cells (n = 122, n = 18, n = 36, n = 18, respectively). ns, not significant.

Table 3. Diagnostic performances of SS phenotypic markers

Criterion	Threshold	Sensitivity (%)	Specificity (%)	PPV (%)	NPV (%)
Ratio CD4/CD8	13	55.6	97.8	66.7	96.4
$CD4^+CD26^-$	28%	94.4	92.8	50.0	99.6
$CD4^+CD26^-$	465/μL	94.4	90.3	43.6	99.5
$CD4^+CD7^-$	66%	27.8	99.6	83.3	94.7
$CD4^+CD7^-$	360/μL	50.0	94.5	40.9	96.1
$CD4^+CD26^-CD158k^+$	12%	77.8	96.3	63.6	98.1
$CD4^+CD26^-CD158k^+$	107/μL	77.8	96.8	66.7	98.1
$CD4^+CD26^-PD\text{-}1^+$	44%	55.6	91.2	37.0	95.7
$CD4^+CD26^-PD\text{-}1^+$	82/μL	100.0	85.5	40.0	100.0

NPV, negative predictive values; PPV, positive predictive values.

the following antibodies: anti–CD3-APCR700, anti–CD26-FITC, anti–CD30-APC, anti–CD279-BV421 (BDBiosciences), anti–CD-158ek-PE (Miltenyi Biotec), anti–CD4-PC7, anti–CD7-PerCP-Cy5.5, anti–CD28-PE-CF594, anti–CD45-BV510 (BioLegend), and anti–CD8-AA750 (Beckman Coulter). Anti–CD158ek-PE was chosen because of its commercial availability. There is no evidence of KIR3DL1 (CD158e) expression on either Sezary cells or normal T $CD4^+$.[14] Anti–T-cell receptor (TCR)-Vβ antibodies (Beckman Coulter) were used when clonal circulating cells were suspected. Red blood cells were lysed with BD FACS Lysing Solution (BDBiosciences). Acquisition of a minimum of 50 000 T cells was performed using Navios Flow Cytometer (Beckman Coulter). Counting beads were used for absolute values assessment (FlowCount Fluorospheres; Beckman Coulter). Data were analyzed using Kaluza software (Beckman Coulter).

Multivariate analysis

Computational analysis of lymphocytes was performed using FlowSOM method in R plug-in on Kaluza as described by Lacombe et al.[15] Briefly, for the antibody combination, all listmode (lmd) files were processed using the FlowSOM module (Bioconductor version 3.3.2 with flowSOM and flowCore packages) integrated to the analysis software Kaluza (Beckman Coulter). In a first step,

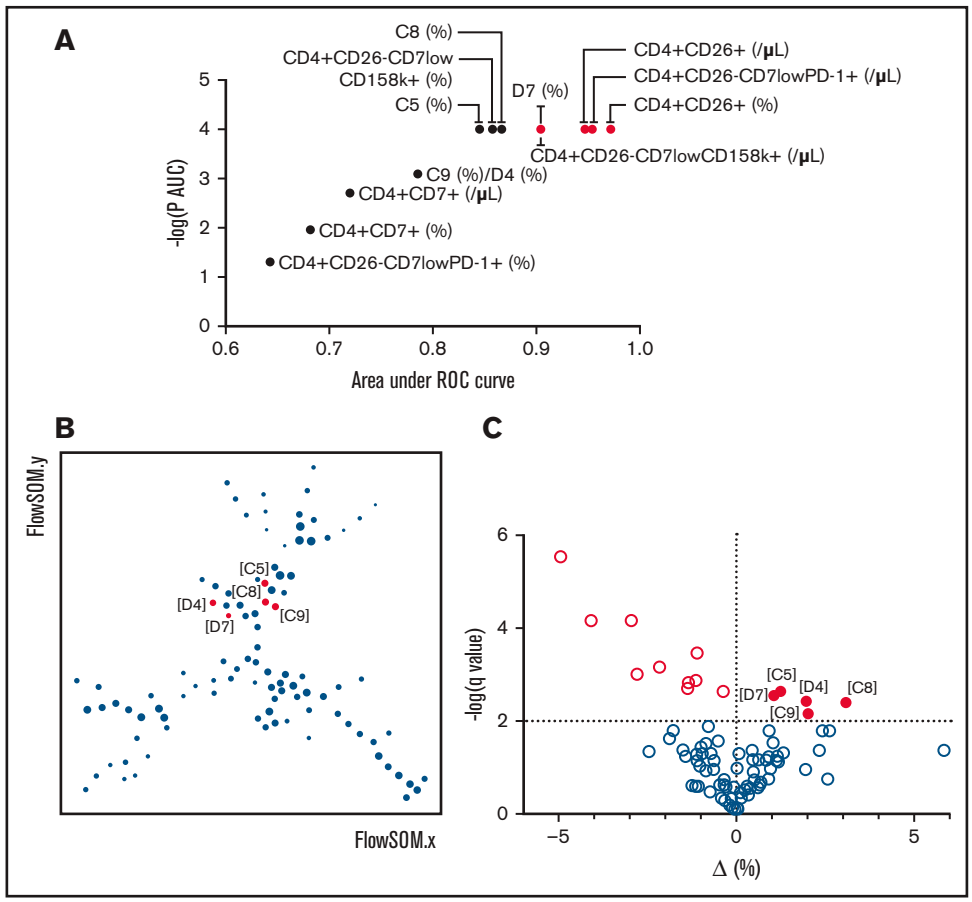

Figure 2. Univariate and multivariate diagnostic performances of FC data in SS. (A) −log(P) of ROC curves as a function of AUC for each parameter of interest. Red dots represent parameters with AUC ≥ 0.9 and high discriminating power between SS and non-patients with SS ($P < .0001$), which are considered the best parameters for SS diagnosis. Classical FCM parameters are represented ($CD4^+CD26^-$, $CD4^+CD7^-$, $CD4^+CD26^-CD158k^+$, and $CD4^+CD26^-PD\text{-}1^+$) as well as new parameters obtained with the multivariate analysis method using the FlowSOM algorithm (C5, C8, C9, D4, and D7). (B) Best SS seed obtained with unsupervised multivariate analysis of the lmd file of merged SS using the FlowSOM algorithm. Cells are clustering according to their phenotype. Node size is proportionate to cell number. Red dots represent nodes of interest for SS diagnosis. (C) Volcano plot of SS (n = 18) vs non-CTCL (n = 35). Red rings represent nodes overrepresented in non-CTCL patients, red dots represent nodes overrepresented in patients with SS (called C5, C8, C9, D4, and D7).

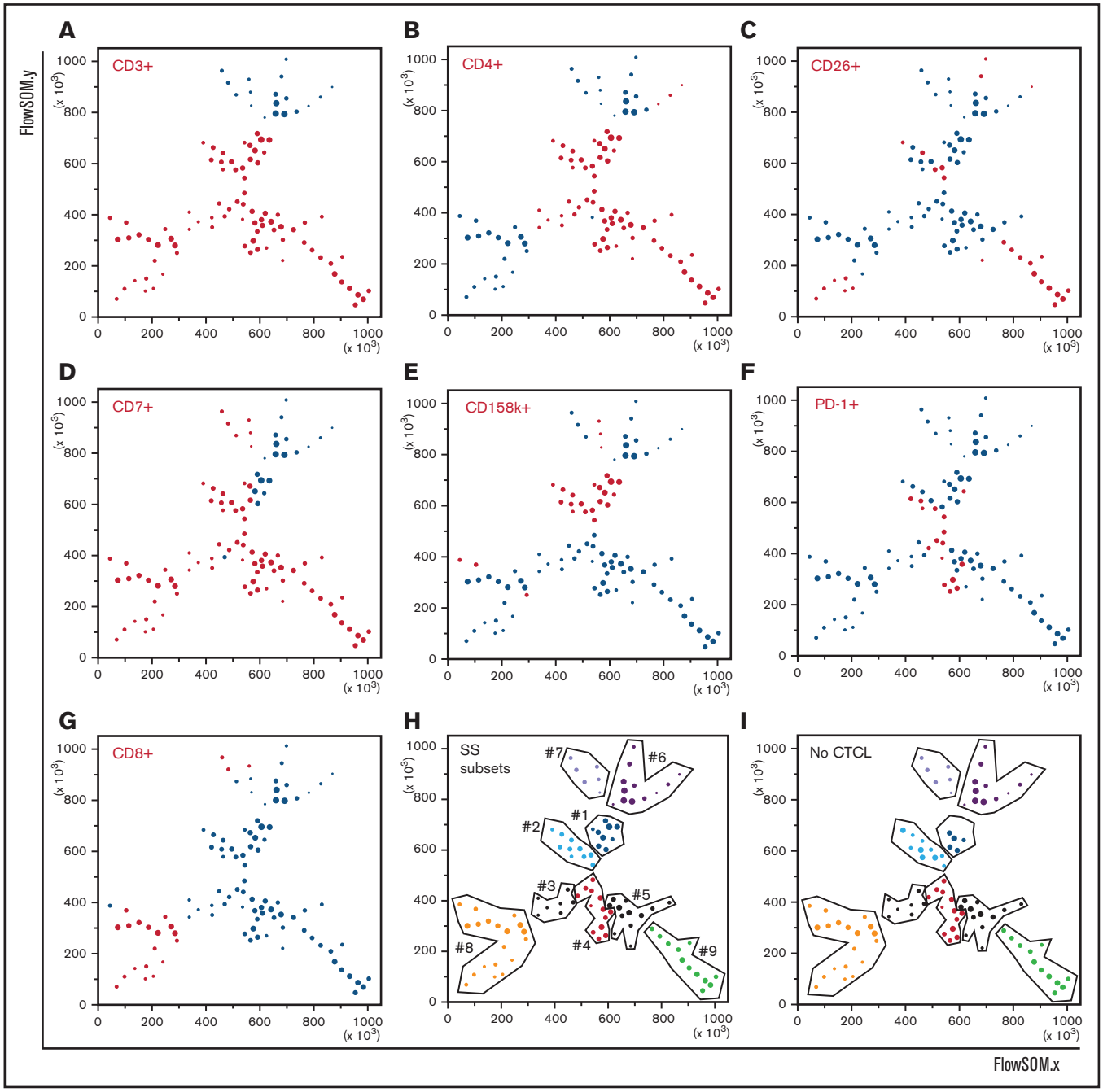

Figure 3. FlowSOM nodes phenotypes define different subsets. (A) CD3 expression on different SS nodes (when a marker is expressed on cells, node appears in red). (B) CD4 expression. (C) CD26 expression. (D) CD7 expression. (E) CD158k expression. (F) PD-1 expression. (G) CD8 expression. (H) Different subsets of nodes, defined by expression profile of CD4, CD26, CD7, CD158k, and PD-1 (see Table 4 for subset identification). (I) The frozen FlowSOM MST applied to lymphocytes from merged non-CTCL patients lmd files.

compensations were checked, and the 12 parameters of each lmd file were normalized. Normalized files of the 18 SS were then merged and processed to obtain a frozen reference minimal spanning tree (MST) of 100 nodes. The lmd file of merged SS was then processed together with the normalized 35 merged controls (non-CTCL) and, one by one, each normalized SS lmd file for each patient, in the FlowSOM module. As in other diseases, FlowSOM method allows a clear and visual representation of how all markers are behaving on all cells.[16]

Pathological analysis

Sixteen skin biopsies were blindly reviewed, without considering cytometry data. Several parameters were evaluated: distribution

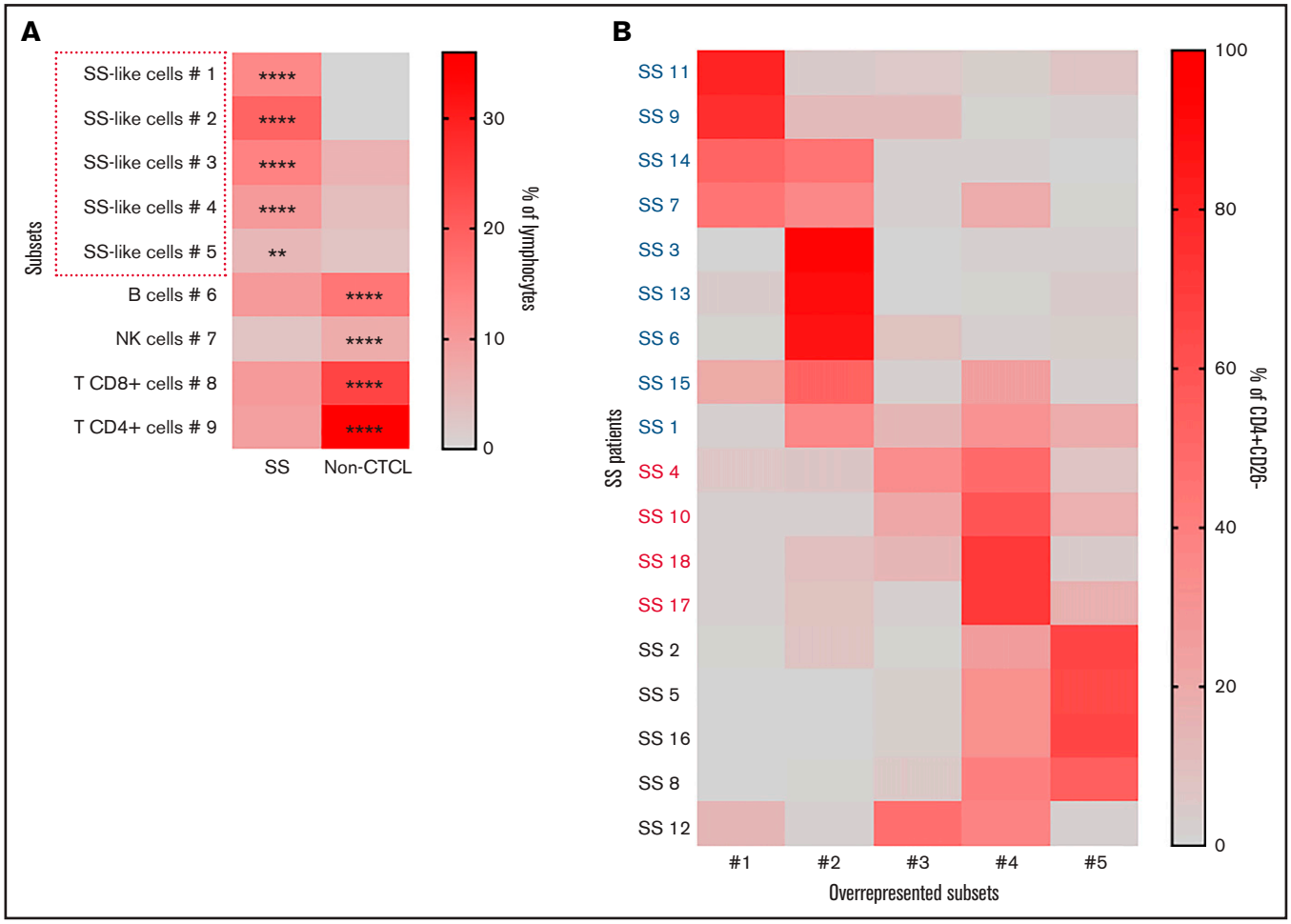

Figure 4. SS subsets of interest. (A) Heat map of subset distribution (% of lymphocytes) in patients with SS (n = 18) and non-CTCL patients (n = 35). Each row corresponds to a subset of lymphocytes. Subset distribution is different between patients with SS and non-CTCL patients (2-way ANOVA; $P < .0001$). Five subsets (red box) are significantly overrepresented in patients with SS (Sidak's multiple comparison test). (B) Subset distribution in each patient with SS. Each row corresponds to 1 patient with SS and shows the proportion of each subset of interest (% $CD4^+CD26^-$). Three SS classes were defined by the type of majority subset: blue font corresponds to $CD158k^+$ SS (majority of 1 or 2); red corresponds to $CD158k^-PD\text{-}1^+$ SS (majority of 4), and black corresponds to $CD158k^-PD\text{-}1^-$ SS (majority of 3 or 5).

and density of the lymphoid infiltrate, size of tumor cells, epidermal associated changes, cellular environment (eosinophils, plasma cells, reactive $CD19^+$ B cells, and reactive $CD8^+$ T cells), and PD-1 expression and intensity on tumor cells. A semi-quantitative estimation of the number of B cells compared with the whole infiltrate (0: no B cells; 1: <5%; 2: >5%) and of $CD8^+$ T cells compared with $CD3^+$ cells (0: no $CD8^+$ cells; 1: <10%; 2: >10%) was done.

Statistical analysis

Comparisons were performed using a Mann-Whitney test or Kruskal-Wallis test for continuous variables and Fisher's exact test,

Table 4. Subset characteristics

Subsets	Phenotype	Identification	Nodes	SS (% IQR)	Non-CTCL (% IQR)
1	$CD4^+CD26^-CD7^-CD158k^+PD\text{-}1^-$	SS-like cells	9	70.4	7.6
2	$CD4^+CD26^-CD7^+CD158k^+PD\text{-}1lo$	SS-like cells	10	83.2	20.8
3	$CD4^+CD26^-CD7^-CD158k^-PD\text{-}1lo$	SS-like cells	7	42.3	16.8
4	$CD4^+CD26^-CD7^+CD158k^-PD\text{-}1hi$	SS-like cells	13	36.2	20.7
5	$CD4^+CD26^-CD7^+CD158k^-PD\text{-}1^-$	SS-like cells	12	62.2	10.3
6	$CD4^-CD26^-CD7^-CD158k^-PD\text{-}1^-$	B cells	12	37.9	45.3
7	$CD4^-CD26^-CD7^+CD158k^{-/+}PD\text{-}1^-$	NK cells	6	17.2	34.0
8	$CD4^-CD26^-CD7^+CD158k^-PD\text{-}1^-$	T $CD8^+$ cells	19	37.3	53.4
9	$CD4^+CD26^+CD7^+CD158k^-PD\text{-}1^-$	T $CD4^+$ cells	12	34.8	59.3

Table 5. *z* score MFI mean of subsets of interest

	1		2		3		4		5	
	Mean	SD	Mean	SD	Mean	SD	Mean	SD	Mean	SD
CD4	−0.35	0.24	0.56	0.28	0.89	0.41	0.67	0.69	0.59	0.37
CD26	−0.49	0.01	−0.34	0.14	−0.47	0.03	−0.42	0.04	−0.39	0.14
CD7	−1.15	0.08	−0.33	0.29	−1.00	0.11	0.43	0.54	0.07	0.30
CD158k	1.00	0.24	1.86	0.43	−0.51	0.10	−0.46	0.07	−0.55	0.06
PD-1	0.20	0.57	0.75	0.89	0.55	0.72	1.37	0.69	−0.69	0.90

χ^2 test, or 1-way analysis of variance (ANOVA) or 2-way ANOVA for categorical variables with GraphPad Prism. Statistical test results are graphically expressed: *$P \leq .05$, **$P \leq .01$, ***$P \leq .001$, ****$P \leq .0001$.

Results

Cohort validation according to the ISCL criteria

Peripheral blood cells from 231 patients (18 SS, 39 MF, 18 other types of CTCL [Table 2],[17] and 156 non-CTCL) were analyzed for CD4/CD8 ratio and $CD4^+$ T-cell expression of CD26 and CD7. In agreement with the literature and ISCL criteria, CD4/CD8 ratio, the percentages and absolute values of $CD4^+CD26^-$ T cells and $CD4^+CD7^-$ T cells were significantly increased in the 18 patients with SS.[3,4,18,19] The CD4/CD8 ratio was 7 times higher in patients with SS (mean = 27.2; interquartile range [IQR] = 24.4) compared with the non-CTCL group (mean = 3.7, IQR = 2.7; Figure 1A). The percentage of $CD4^+CD26^-$ lymphocytes was 5 times higher in patients with SS (mean = 60.9; IQR = 48.8) compared with the non-CTCL group (mean = 12.7; IQR = 6.0; Figure 1B). The percentage of $CD4^+CD7^-$ lymphocytes was 5 times higher in patients with SS (mean = 27.7; IQR = 70.35) compared with the non-CTCL group (mean = 6.0, IQR = 5.0; Figure 1C).

Then, we determined thresholds with the Fayyad and Irani method for each criterion (SS vs no SS).[20] Despite the small size of the SS cohort, we found similar thresholds as defined in the literature except for the percentage of lymphocytes of $CD4^+CD7^-$ (Table 3).[3,4] For this parameter, we obtained a threshold of 66% with the Fayyad and Irani method, whereas the ISCL threshold is set at 40%.

As expected, our data showed excellent sensitivity (>90%) and specificity (>90%) for the threshold of 27.5% $CD4^+CD26^-$ cells (30% according to the ISCL criteria).[21] There was an excellent specificity for the threshold of 66% $CD4^+CD7^-$ cells and the threshold of 12.7 for the CD4/CD8 ratio but an obvious lack of sensitivity (Table 3). Negative predictive values were >94% for all criteria, but positive predictive values were low, certainly because of the size of the SS cohort. In this cohort, the percentage of $CD4^+CD26^-$ cells was the best performing marker among the classical ISCL criteria (area under the receiver operating characteristic [ROC] curve [AUC] = 0.9723; Figure 2A). At the opposite extreme, the percentage of $CD4^+CD7^-$ was the least powerful marker among the classical ISCL criteria to diagnose SS (AUC = 0.6799; Figure 2A).

These results validated the cohort and allowed us to explore new markers and a new analysis method.

Evaluation of coexpression of additional phenotypic SS markers

Concomitantly, peripheral blood cells were analyzed for the expression of CD158k and PD-1/CD279 on Sezary-like $CD4^+CD26^-$ cells in order to improve the sensitivity and specificity of the already effective $CD4^+CD26^-$ criterion. Classical supervised dot-plot analysis was performed. As expected, we found that the percentage and absolute values of $CD4^+CD26^-CD158k^+$ cells are significantly higher in patients with SS compared with other categories[10] (Figure 1D,H). We observed the same pattern regarding PD-1 expression even if there were more overlapping phenotypes between the different categories of patients[12] (Figure 1E,I).

With the Fayyad and Irani method, we defined 4 threshold values with the best SS diagnostic performances[20] (Table 3).

The threshold for absolute $CD4^+CD26^-CD158k^+$ cells values of 107/μL showed a sensitivity of 77.8% and a specificity of 96.4%, making it the most specific univariate marker with acceptable sensitivity (AUC = 0.9050; Table 3; Figure 2A).

The threshold for absolute of $CD4^+CD26^-PD\text{-}1^+$ cell values of 82/μL showed a sensitivity of 100% and a specificity of 84%, making it the most sensitive marker in our study but with a persistent lack of specificity (AUC = 0.9537; Figure 2A).

FlowSOM unsupervised multivariate analyses of phenotypic data

These data led us to combine different markers in a multivariate model to improve the diagnostic performance of FC. For this purpose, we used the FlowSOM algorithm.

Gated lymphocyte phenotypic data of 18 patients with SS and 35 non-CTCL patients were included in the model.

The FlowSOM algorithm allowed for cells to be clustered according to their phenotype.

First, the best seed of nodes, allowing the best cell separation was generated on merged SS files (Figure 2B).

To evaluate the specificity of FlowSOM nodes, we compared their frequency to those from 35 non-CTCL patients. Using a volcano plot and multiple Student *t* tests, we identified 15 nodes of interest among 100 nodes, including 5 nodes significantly ($P < .01$) overrepresented in patients with SS (Figure 2C; supplemental Figure 1).

Using the ROC curve, we studied diagnostic performances of each node overrepresented in patients with SS. The 5 selected nodes, even cumulated, do not show better performances than the classical ISCL criteria (Figure 2A).

To characterize those nodes overrepresented in patients with SS, we studied the median fluorescence intensities of CD4, CD26, CD7, CD158k, and PD-1 (supplemental Figure 2). We observed that there is no unique profile; each node showed a variable expression of CD4, CD26, CD7, CD158k, and PD-1.

Then, considering heterogeneity and the performance diagnostic of individual nodes of interest, we decided to classify the nodes into different subsets according to their common expression profile.

The expression of the markers was highlighted on frozen FlowSOM MST graphs to delineate different subsets of lymphocytes (Figure

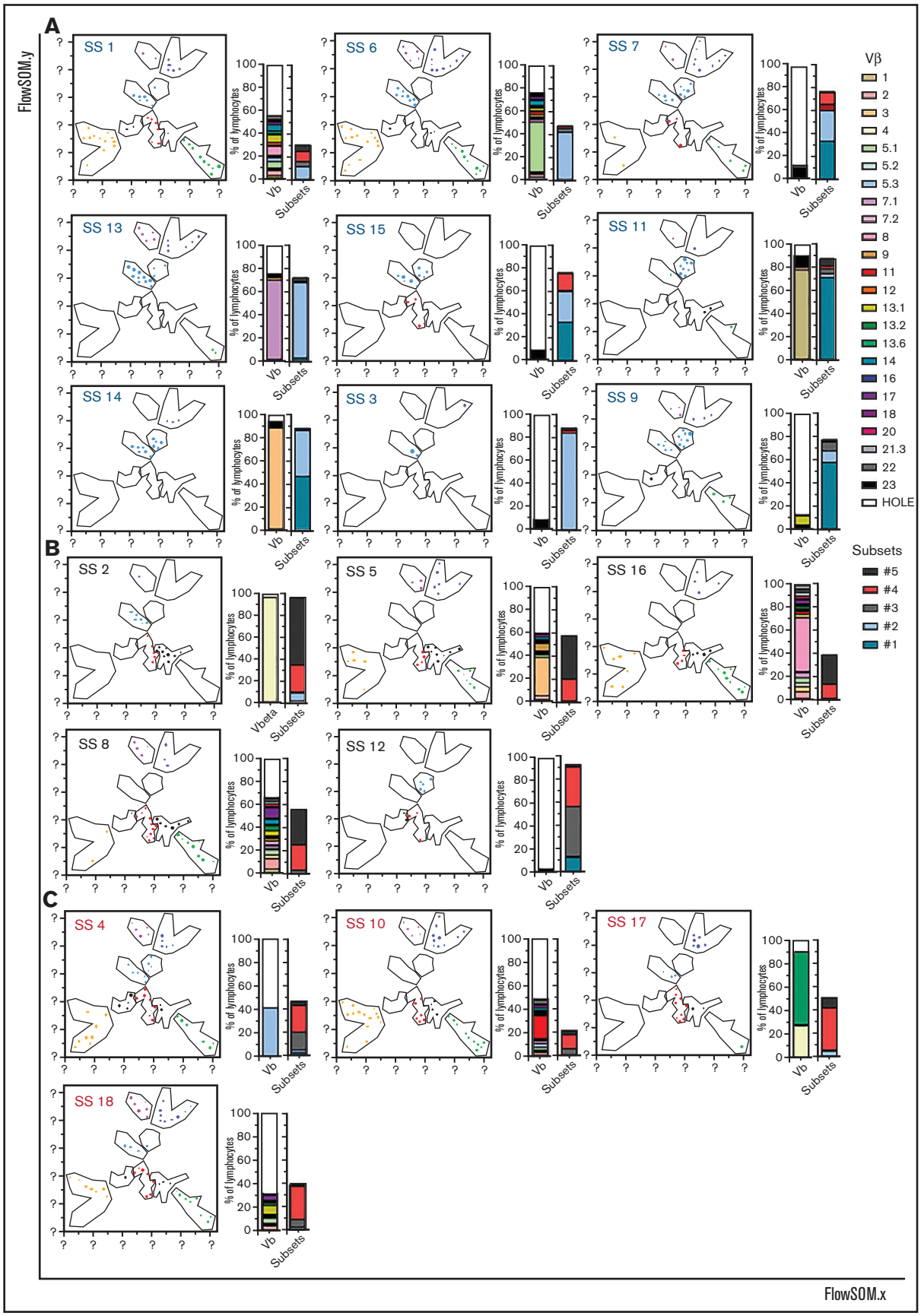

Figure 5. Clonality assessment of T cells by FC. Patients with SS were screened for TCRVβ repertoire restriction by FC. Each frozen FlowSOM of a patient with SS is represented next to the repartition of its TCRVβ repertoire and the 5 subsets of interest (% of lymphocytes). (A) Patients with SS with a CD158k^{+} profile (predominantly subsets 1 or 2, n = 9). (B) Patients with SS with a CD158k^{-}PD-1^{-} profile (predominantly subsets 3 or 5; n = 5). (C) Patients with SS with a CD158k^{-}PD-1^{+} profile (predominantly subset 4; n = 4).

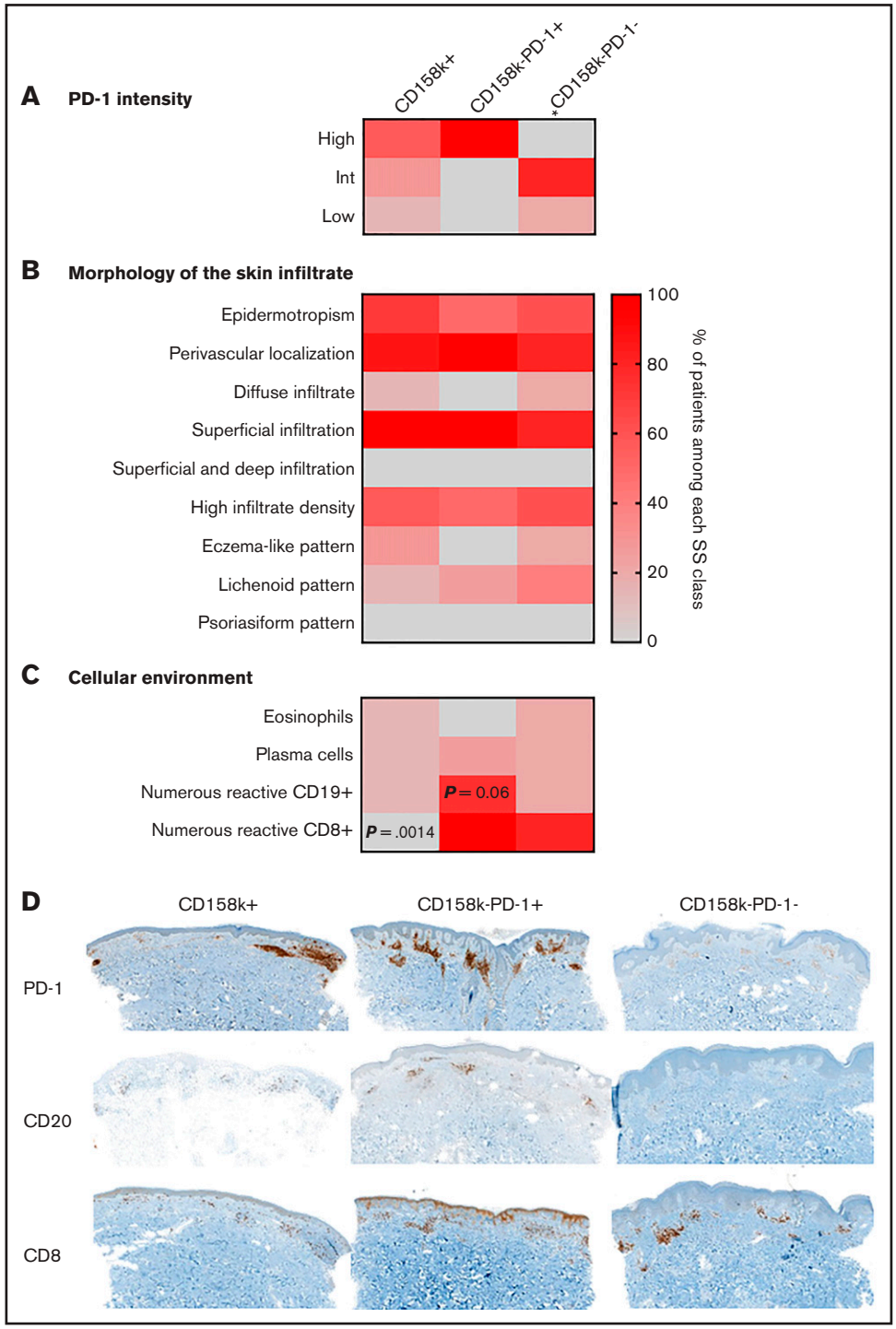

Figure 6. SS class characterization in skin biopsies. (A) Heat map of the PD-1 intensity of expression according to the 3 different phenotypic profiles. Each row corresponds to an intensity and percentage of patients among each SS class who show this intensity. Patient distribution among PD-1 intensity is significantly different in the CD158k$^-$PD-1 class compared with the 2 other classes (χ^2 test, $P = .024$). (B) Heat map related to the morphology of the skin infiltrate. Each row corresponds to a morphologic characteristic and percentage of patients among each SS class who show this characteristic. (C) Heat map related to the cellular environment. It represents the percentage of patients within each SS class for which the presence of different cell types is observed (Fisher exact test). (D) Skin biopsies of different patients with SS showing difference of expression between the 3 phenotypic classes for CD20, CD8, and PD-1. From left to right and top to bottom: CD158k$^+$ profile, CD20 (patient 20T45075, ×6.3); CD158k$^-$PD-1$^+$ profile, CD20 (patient 16T32744, ×6.2); CD158k$^-$PD-1$^-$ profile, CD20 (patient 16T844, ×7.9); CD158k$^+$ profile, CD8 (patient 17t026310, ×7.5); CD158k$^-$PD-1$^+$ profile, CD8 (patient 16T28107, ×6.3); CD158k$^-$PD-1$^-$ profile, CD8 (patient 16T844, ×7.1); CD158k$^+$ profile, PD-1 (patient 17T026310, ×6.3); CD158k$^-$PD-1$^+$ profile, PD-1 (patient 16T28107, ×5.8); CD158k$^-$PD-1$^-$ profile, PD-1 (patient 16T844PD1, ×5.3). Int, intermediate.

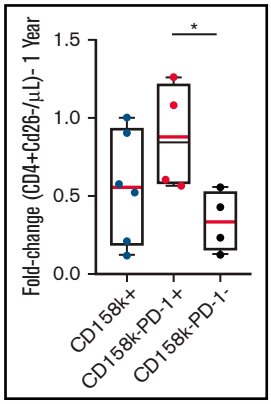

Figure 7. $CD4^+CD26^-$ absolute value course for each patient with SS during follow-up. The histogram represents fold changes of the absolute count of $CD4^+CD26^-$ cells during a year (365 ± 50 days) of each patient with enough data (n = 14) according to each phenotypic profile.

3A-F, supplemental Figure 3). Nine subsets of nodes were defined according to their expression profile (Figure 3G).

The frozen FlowSOM MST and subsequently defined subsets of nodes were also applied to lymphocytes from merged non-CTCL patient lmd files and compared with those from patients with SS (Figure 3H). Five overrepresented subsets of nodes were identified in patients with SS (2-way ANOVA, $\alpha = 0.05$; Sidak multiple comparison test) (Figure 4A).

As expected, the subsets were $CD4^+$ T cells repressing the expression of CD26. Specifically, 2 subsets of 19 nodes strongly expressed CD158k (*z* score mean fluorescence intensity [MFI] mean ≥1) (subsets 1 and 2), and 1 subset of 13 nodes highly expressed only PD-1 (*z* score MFI mean ≥1) (subset 4) (Figure 3; supplemental Figure 3; Table 5). CD7 expression was heterogeneous (Figure 3; supplemental Figure 3; Tables 3 and 4).

Different classes of SS

In order to study the phenotypic profiles of SS, we focused on the 51 nodes of the 5 identified subsets. We classified the 18 SS according to the frequency of nodes in each subset: 4 patients overexpressed subset 1; 5 patients overexpressed subset 2; 1 patient overexpressed subset 3; 4 patients overexpressed subset 4; and 4 patients overexpressed subset 5, demonstrating high heterogeneity (Figure 4B).

We defined 3 phenotypic classes of SS: $CD158k^+$ SS (majority of subsets 1 and 2), $CD158k^-PD\text{-}1^+$ SS (majority of subset 4), CD158k, and PD-1 double-negative SS (majority of subsets 3 and 5) (Figure 4B).

It is worth noting that clonal proliferation of T-cell lymphoma was phenotypically evaluated by measuring the expression of the TCR Vβ repertoire.[22] Among the 18 patients, we identified a TCR Vβ clone in 56% (10/18) and a hole in the TCR repertoire in 33% (6/18). We confirmed the correlation between the Vβ clone or the repertoire hole proportion and the predominant subset proportion in each patient, although the predominant subset does not represent all the Vβ clone (Figure 5; supplemental Figure 4).

To complete the characterization of the different phenotypic classes of SS, diagnostic skin biopsies of 16 patients were blindly reviewed (Figure 6).

The immunohistochemical expression of PD-1 by SS cells correlated with the phenotypic classes (Figure 6A). The study of the cellular environment showed that the $CD158k^+$ profile had significantly (Fisher exact test, $P < .05$) less reactive $CD8^+$ T cells in the skin, and the $CD158k^-PD\text{-}1^+$ profile appeared to have more reactive $CD19^+$ cells (Fisher exact test; $P = .06$). To summarize, we identified 3 SS classes according to their cellular environment in correlation with the 3 phenotypic profiles (Figure 6C-D).

Interestingly, the study of circulating cells showed that the $CD158k^-PD\text{-}1^+$ SS class had significantly more circulating B cells (supplemental Figure 4). There was no significant difference considering circulating $CD8^+$ T cells, but they were threefold increased in the $CD158k^-PD\text{-}1^+$ class, without reaching statistical significance ($P = .09$), certainly because of the low number of patients (supplemental Figure 5). The results were therefore similar between skin and blood.

Phenotypic profiles of SS are stable during treatment and could be used to monitor minimal residual circulating disease

Because we identified 3 classes of SS with heterogeneous immune profiles, we wondered if they could correlate with treatment response.

Biological follow-up of patients with SS was monitored in blood by measuring the level of $CD4^+$ SS cells (ie, $CD26^-$ or $CD7^-$).[3] To evaluate whether CD158k or PD-1 could be used as an SS cell readout, we followed their expressions during treatment. Whereas lymphocyte count fluctuated, the phenotype of SS cells was stable in all SS classes (supplemental Figure 6). Therefore, the residual circulating disease could be efficiently evaluated by absolute count of SS cells that could be identified by their expressions of CD158k and PD-1 at diagnosis[4] and that were consistently and robustly expressed during treatment.

We evaluated the treatment response as the absolute value of SS $CD4^+CD26^-$ cells. In the SS cohort, at the 1-year follow-up evaluation, the absolute count of $CD4^+CD26^-$ cells in the $CD158k^-PD1^-$ class decreased 1.6 times more than that of the $CD158k^+$ class and significantly 2.5 times more than that of the $CD158k^-PD\text{-}1^+$ class (Figure 7). The absolute count of $CD4^+CD26^-$ cells in the $CD158k^+$ class decreased 1.5 times more than that of the $CD158k^-PD\text{-}1^-$ class without reaching statistical significance (Figure 7).

Discussion

The first step was to validate our cohort. This step was important because of the SS cohort size, which could bias statistical analyses. Indeed, it was a small cohort of fresh samples, but comparable to what has already been described in the literature (eg, 16 blood and skin-paired samples of patients with SS).[5,8,23-25] In contrast, our non-CTCL cohort is substantial and allowed us to define reliable diagnostic thresholds. We therefore began by studying the classical ISCL criteria. As described, measurement of $CD4^+CD26^-$ cells

percentage was the most reliable marker but could not be used as a stand-alone diagnostic criterion because 5.5% of non-CTCL patients (9 on 156) had a value above the 30% ISCL threshold. It should be noted that CD7 loss is not sensitive enough in our cohort. We defined a threshold of 66% for the $CD4^+CD7^-$ percentage compared with 40% in the literature. This difference could be explained by the fact that CD7 loss is frequently associated with cell senescence and that the percentage of $CD4^+CD7^-$ cells increases with age.[26,27] Therefore, the percentage of $CD4^+CD7^-$ cells may vary in non-CTCL patients depending on the age of the patients. Furthermore, expansion of $CD4^+CD7^-$ cells may also be observed in reactive dermatoses.[28] In addition, CD7 loss is also described in other T-cell neoplasms, which we have included to calculate the thresholds in our study.[29] Finally, as described in the literature, CD7 expression depends on the stage of the disease.[30] Considering those data, $CD4^+CD7^-$ percentage, although considered a classical feature of CTCL, should be used with caution in SS diagnosis.

Once our cohort validated, the first aim of the study was to evaluate CD158k and PD-1/CD279 coexpression for the diagnosis of SS. We showed a significant increase of $CD4^+CD26^-CD158k^+$ cells and $CD4^+CD26^-PD\text{-}1^+$ cells in patients with SS compared with other patients. We defined thresholds for percentages and absolute values with good diagnostic performances. CD158k is highly discriminating with only 3.7% of patients without CTCL (6 on 156) expressing SS-like $CD158k^+$ cells above the threshold of 100/μL. These data confirm previous reports.[10,21] It can be noted that we found a slightly lower threshold in our cohort. This may be due to a different gating strategy or a difference between the patients included in the control group.[21] These results also confirm that the anti-CD158ek (commercially available) can be incorporated in FC panels for the diagnosis of SS. PD-1 is extremely sensitive but lacks specificity probably because it is an activation and exhaustion marker also expressed by normal lymphocytes during aging.[31,32]

The second and major aim of our study was to evaluate the interest of using unsupervised multivariate analysis in SS diagnosis. Multivariate analysis allowed for the simultaneous study of markers of interest, such as CD158k and PD-1 on SS cells, with has never been described to our knowledge. This method allowed for the identification of SS cells, distributed heterogeneously in 5 subsets of nodes. It was an easy way to evaluate blood involvement by SS cells, as their phenotype was unchanged during follow-up. Moreover, if the phenotype realized at diagnosis is available, this type of representation allows a better sensitivity and could be used to assess minimal residual disease, as in other disease.[16] With this method, we could also easily imagine adding other markers to increase analytic performances and refine diagnosis.

In an interesting way, using multivariate analysis, we identified 3 classes of SS according to their phenotypic profile, which had never been described to our knowledge: $CD158k^+$, $CD158k^-PD\text{-}1^+$, and $CD158k^-PD\text{-}1^-$ SS.

In light of this discovery, we tried to characterize these 3 classes.

For this purpose, we compared our data with pathological data from skin biopsies. We observed that there was no significant difference between patients with SS regarding cutaneous lymphoma infiltration, but there were notable differences regarding the cellular environment (B cells and $CD8^+$ T cells). The 3 phenotypic classes did not have the same cellular environment, suggesting a different immune response to tumor cells or to infections. Interestingly, according to the literature, bacterial sepsis, related to cellular immunity impairment, is the main cause of death in a patient with SS.[33]

Some studies were interested in adaptive immunity in SS involving circulating $CD8^+$ T cells. One recent study showed a chronic activation of $CD8^+$ T cells, with exhaustion marker expression and attenuated cytotoxic profile in patients with SS.[34] Another found that $CD8^+$ T cells downregulate the growth of tumor cells.[35,36] Moreover, high density of $CD8^+$ T-cell infiltrate is associated with a more favorable prognosis.[37] This could explain the better treatment response of $CD158k^-PD\text{-}1^-$ patients with SS in which numerous $CD8^+$ T cells were observed in skin biopsies. In particular, photosensitive lesions are characterized by a $CD8^+$ T-cell–dominant infiltrate, so a phenotypic profile with more $CD8^+$ T cells in the skin could be a better responder to phototherapy.[38]

In contrast, there is no literature reporting the involvement of B cells in immune response in SS. We know that T follicular helper cells play a role in stimulating B-cell response.[39] $CD158k^-PD\text{-}1^+$ SS cells show a T follicular helper–like profile with a strong expression of PD-1; interestingly, we found in the skin biopsies of those patients a high $CD19^+$ infiltrate.[39] The impact of B-cell expansion on the outcome of patients with SS remains to be determined.

Regarding PD-1 expression, its immunosuppressive nature makes it an interesting therapeutic target in SS.[12] The existence of 3 SS classes with variable intensity of expression could eventually predict the outcome and/or response to different therapies, including anti-PD-1.[12,40]

Obviously, further studies on larger cohorts are necessary to better define these different profiles, but there appear to be several subtypes of SS with different biological behavior especially with respect to the tumor microenvironment.

The need for surrogate biomarkers such as tumor environment has already been discussed to help distinguish patients for whom ECP monotherapy is sufficient from those who may benefit from ECP in combination with other agents.[41] To further investigate this question, it would be interesting to compare responses to treatment between each SS class. Such a study could help to define biological markers of susceptibility/resistance to treatment, including ECP or immunotherapy (eg, anti-KIR3DL2).[42] Then, phenotypic profiles could help to choose better targeted therapy for a patient.

Authorship

Contribution: I.V. analyzed the data and wrote the paper; C.D.-B. collected and integrated the data; S. Boulinguez provided clinical data and followed patients; J.-B.R. and J.-P.V. helped to write the paper; R.B., S. Boudot, A.C., S.C., M.D., S.E., N.L., and M.-L.N.-T. performed the cytometry analysis; E.T. performed pathological analysis; L.L. performed pathological analysis and helped to write the

paper; and F.V. designed research, analyzed the data, and wrote the paper.

Conflict-of-interest disclosure: The authors declare no competing financial interests.

ORCID profiles: J.-B.R., 0000-0002-0950-979X; J.-P.V., 0000-0003-3109-0064; F.çoisV., 0000-0002-0063-4404.

Correspondence: Inès Vergnolle, Laboratoire d'Hématologie, Institut Universitaire du Cancer de Toulouse Oncopole, 1 Ave Irène Joliot-Curie, 31059 Toulouse Cedex 9, France; e-mail: vergnolle.ines@iuct-oncopole.fr; and François Vergez, Laboratoire d'Hématologie, Institut Universitaire du Cancer de Toulouse Oncopole, 1 Ave Irène Joliot-Curie, 31059 Toulouse Cedex 9, France; e-mail: vergez.francois@iuct-oncopole.fr.

References

1. Dulmage B, Geskin L, Guitart J, Akilov OE. The biomarker landscape in mycosis fungoides and Sézary syndrome. *Exp Dermatol.* 2017;26(8):668-676.
2. Pulitzer MP, Horna P, Almeida J. Sézary syndrome and mycosis fungoides: an overview, including the role of immunophenotyping. *Cytometry B Clin Cytom.* 2021;100(2):132-138.
3. Scarisbrick JJ, Hodak E, Bagot M, et al. Blood classification and blood response criteria in mycosis fungoides and Sézary syndrome using flow cytometry: recommendations from the EORTC cutaneous lymphoma task force. *Eur J Cancer.* 2018;93(93):47-56.
4. Olsen E, Vonderheid E, Pimpinelli N, et al; ISCL/EORTC. Revisions to the staging and classification of mycosis fungoides and Sezary syndrome: a proposal of the International Society for Cutaneous Lymphomas (ISCL) and the cutaneous lymphoma task force of the European Organization of Research and Treatment of Cancer (EORTC). *Blood.* 2007;110(6):1713-1722.
5. Roelens M, Delord M, Ram-Wolff C, et al. Circulating and skin-derived Sézary cells: clonal but with phenotypic plasticity. *Blood.* 2017;130(12):1468-1471.
6. Campbell JJ, Clark RA, Watanabe R, Kupper TS. Sezary syndrome and mycosis fungoides arise from distinct T-cell subsets: a biologic rationale for their distinct clinical behaviors. *Blood.* 2010;116(5):767-771.
7. Scala E, Narducci MG, Amerio P, et al. T cell receptor-Vbeta analysis identifies a dominant $CD60^{+}$ CD26 CD49d T cell clone in the peripheral blood of Sézary syndrome patients. *J Invest Dermatol.* 2002;119(1):193-196.
8. Buus TB, Willerslev-Olsen A, Fredholm S, et al. Single-cell heterogeneity in Sézary syndrome. *Blood Adv.* 2018;2(16):2115-2126.
9. Nicolay JP, Felcht M, Schledzewski K, Goerdt S, Géraud C. Sézary syndrome: old enigmas, new targets. *J Dtsch Dermatol Ges.* 2016;14(3):256-264.
10. Moins-Teisserenc H, Daubord M, Clave E, et al. CD158k is a reliable marker for diagnosis of Sézary syndrome and reveals an unprecedented heterogeneity of circulating malignant cells. *J Invest Dermatol.* 2015;135(1):247-257.
11. Cetinözman F, Jansen PM, Vermeer MH, Willemze R. Differential expression of programmed death-1 (PD-1) in Sézary syndrome and mycosis fungoides. *Arch Dermatol.* 2012;148(12):1379-1385.
12. Samimi S, Benoit B, Evans K, et al. Increased programmed death-1 expression on $CD4^{+}$ T cells in cutaneous T-cell lymphoma: implications for immune suppression. *Arch Dermatol.* 2010;146(12):1382-1388.
13. Duetz C, Bachas C, Westers TM, van de Loosdrecht AA. Computational analysis of flow cytometry data in hematological malignancies: future clinical practice? *Curr Opin Oncol.* 2020;32(2):162-169.
14. Ortonne N, Le Gouvello S, Mansour H, et al. CD158K/KIR3DL2 transcript detection in lesional skin of patients with erythroderma is a tool for the diagnosis of Sézary syndrome. *J Invest Dermatol.* 2008;128(2):465-472.
15. Lacombe F, Dupont B, Lechevalier N, Vial JP, Béné MC. Innovation in flow cytometry analysis: a new paradigm delineating normal or diseased bone marrow subsets through machine learning. *HemaSphere.* 2019;3(2):e173.
16. Vial JP, Lechevalier N, Lacombe F, et al. Unsupervised flow cytometry analysis allows for an accurate identification of minimal residual disease assessment in acute myeloid leukemia. *Cancers (Basel).* 2021;13(4):629.
17. Willemze R, Cerroni L, Kempf W, et al. The 2018 update of the WHO-EORTC classification for primary cutaneous lymphomas. *Blood.* 2019;133(16):1703-1714.
18. Vonderheid EC, Hou JS. $CD4^{+}CD26^{-}$ lymphocytes are useful to assess blood involvement and define B ratings in cutaneous T cell lymphoma. *Leuk Lymphoma.* 2018;59(2):330-339.
19. Bernengo MG, Novelli M, Quaglino P, et al. The relevance of the $CD4^{+}$ $CD26^{-}$ subset in the identification of circulating Sézary cells. *Br J Dermatol.* 2001;144(1):125-135.
20. Fayyad U, Irani K. Multi-interval discretization of continuous-valued attributes for classification learning. *Proc. 13th Int. Jt. Conf. Artif. Intell. IJCAI-93.* 1993;1022-1027.
21. Roelens M, de Masson A, Ram-Wolff C, et al. Revisiting the initial diagnosis and blood staging of mycosis fungoides and Sézary syndrome with the KIR3DL2 marker. *Br J Dermatol.* 2020;182(6):1415-1422.
22. Feng B, Jorgensen JL, Jones D, et al. Flow cytometric detection of peripheral blood involvement by mycosis fungoides and Sézary syndrome using T-cell receptor Vbeta chain antibodies and its application in blood staging. *Mod Pathol.* 2010;23(2):284-295.

23. Amatore F, Ortonne N, Lopez M, et al. ICOS is widely expressed in cutaneous T-cell lymphoma, and its targeting promotes potent killing of malignant cells. *Blood Adv.* 2020;4(20):5203-5214.

24. Johnson LDS, Banerjee S, Kruglov O, et al. Targeting CD47 in Sézary syndrome with SIRPαFc. *Blood Adv.* 2019;3(7):1145-1153.

25. Kamijo H, Miyagaki T, Shishido-Takahashi N, et al. Aberrant CD137 ligand expression induced by GATA6 overexpression promotes tumor progression in cutaneous T-cell lymphoma. *Blood.* 2018;132(18):1922-1935.

26. Kukel S, Reinhold U, Oltermann I, Kreysel HW. Progressive increase of $CD7^-$ T cells in human blood lymphocytes with ageing. *Clin Exp Immunol.* 1994;98(1):163-168.

27. Ginaldi L, De Martinis M, Modesti M, Loreto F, Corsi MP, Quaglino D. Immunophenotypical changes of T lymphocytes in the elderly. *Gerontology.* 2000;46(5):242-248.

28. Alaibac M, Pigozzi B, Belloni-Fortina A, Michelotto A, Saponeri A, Peserico A. CD7 expression in reactive and malignant human skin T-lymphocytes. *Anticancer Res.* 2003;23(3B):2707-2710.

29. Jamal S, Picker LJ, Aquino DB, McKenna RW, Dawson DB, Kroft SH. Immunophenotypic analysis of peripheral T-cell neoplasms. A multiparameter flow cytometric approach. *Am J Clin Pathol.* 2001;116(4):512-526.

30. Rappl G, Abken H, Muche JM, et al. $CD4^+CD7$ leukemic T cells from patients with Sézary syndrome are protected from galectin-1-triggered T cell death. *Leukemia.* 2002;16(5):840-845.

31. Fukushima Y, Minato N, Hattori M. The impact of senescence-associated T cells on immunosenescence and age-related disorders. *Inflamm Regen.* 2018;38(1):24.

32. Minato N, Hattori M, Hamazaki Y. Physiology and pathology of T-cell aging. *Int Immunol.* 2020;32(4):223-231.

33. Axelrod PI, Lorber B, Vonderheid EC. Infections complicating mycosis fungoides and Sézary syndrome. *JAMA.* 1992;267(10):1354-1358.

34. Torrealba MP, Manfrere KC, Miyashiro DR, et al. Chronic activation profile of circulating $CD8^+$ T cells in Sézary syndrome. *Oncotarget.* 2017;9(3):3497-3506.

35. Seo N, Tokura Y, Matsumoto K, Furukawa F, Takigawa M. Tumour-specific cytotoxic T lymphocyte activity in Th2-type Sézary syndrome: its enhancement by interferon-gamma (IFN-gamma) and IL-12 and fluctuations in association with disease activity. *Clin Exp Immunol.* 1998;112(3):403-409.

36. Wood GS. Lymphocyte activation in cutaneous T-cell lymphoma. *J Invest Dermatol.* 1995;105(1 suppl):105S–109S.

37. Durgin JS, Weiner DM, Wysocka M, Rook AH. The immunopathogenesis and immunotherapy of cutaneous T cell lymphoma: pathways and targets for immune restoration and tumor eradication. *J Am Acad Dermatol.* 2021;84(3):587-595.

38. Masuda Y, Tatsuno K, Kitano S, et al. Mogamulizumab-induced photosensitivity in patients with mycosis fungoides and other T-cell neoplasms. *J Eur Acad Dermatol Venereol.* 2018;32(9):1456-1460.

39. Rao DA. T cells that help B cells in chronically inflamed tissues. *Front Immunol.* 2018;9:1924.

40. Wu X, Gu Z, Chen Y, et al. Application of PD-1 blockade in cancer immunotherapy. *Comput Struct Biotechnol J.* 2019;17:661-674.

41. Wilcox RA. ECP in the spotLIGHT. *Blood.* 2019;134(16):1275-1277.

42. Bagot M, Porcu P, Marie-Cardine A, et al. IPH4102, a first-in-class anti-KIR3DL2 monoclonal antibody, in patients with relapsed or refractory cutaneous T-cell lymphoma: an international, first-in-human, open-label, phase 1 trial. *Lancet Oncol.* 2019;20(8):1160-1170.